

# Tetramethoxyppyrene-Based Biradical Donors with Tunable Physical and Magnetic Properties

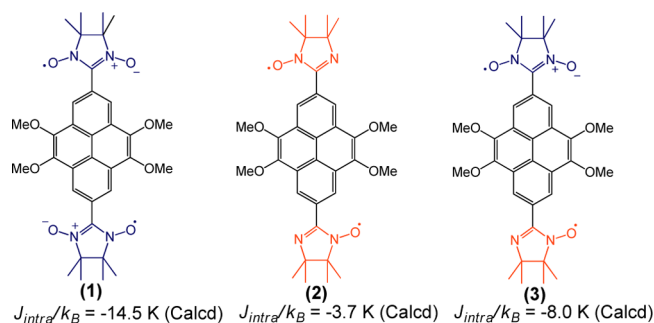
Prince Ravat,<sup>†</sup> Yoshikazu Ito,<sup>†,§</sup> Elena Gorelik,<sup>‡</sup> Volker Enkelmann,<sup>†</sup> and Martin Baumgarten<sup>\*,†</sup>

Max Planck Institute for Polymer Research, Ackermannweg 10, 55128 Mainz, Germany, and Institute of Physics, Johannes Gutenberg-University, Staudingerweg 7, 55128 Mainz, Germany

baumgart@mpip-mainz.mpg.de

Received June 5, 2013

## ABSTRACT



Synthesis of 2,7-disubstituted tetramethoxyppyrene-based neutral biradical donors is reported. The biradicals were characterized by EPR, UV–vis, CV, SQUID, and single-crystal X-ray diffraction, and their optical, electrochemical, and structural properties were compared and discussed. The experimental results are well supported by DFT calculations. Systematic tuning of magnetic exchange interactions was achieved by varying the radical moieties.

In the past decade, the attachment of the stable radical moieties to polyaromatic hydrocarbons has attracted great attention because of their potential for applications in organic field effect transistors (OFETs),<sup>1</sup> sensors,<sup>2</sup> magnetoconducting materials,<sup>3</sup> photoexcited spin systems,<sup>4</sup>

quantum magnets,<sup>5</sup> and batteries.<sup>6</sup> They also have been used as ligands to form metal–organic complexes with transition-metal ions, where ferromagnetism or ferrimagnetism was observed.<sup>7</sup> However, these properties are highly dependent on the type of radical moieties and their positions at the polyaromatic core.<sup>8</sup>

To the best of our knowledge, only C1-substituted pyrene-based (Scheme 1) neutral monoradicals are known; nonetheless, no pyrene-based biradical has been reported<sup>9</sup> to date. Pyrene is a unique example of polyaromatic hydrocarbons with a nodal plane passing through the 2,7

<sup>†</sup> Max Planck Institute for Polymer Research.

<sup>‡</sup> Johannes Gutenberg-University.

<sup>§</sup> WPI Advanced Institute for Materials Research, Tohoku University, Sendai 980-8577, Japan.

(1) (a) Aoki, K.; Akutsu, H.; Yamada, J.-i.; Nakatsuji, S. i.; Kojima, T.; Yamashita, Y. *Chem. Lett.* **2009**, *38*, 112. (b) Figueira-Duarte, T. M.; Müllen, K. *Chem. Rev.* **2011**, *111*, 7260. (c) Wang, Y.; Wang, H.; Liu, Y.; Di, C.-a.; Sun, Y.; Wu, W.; Yu, G.; Zhang, D.; Zhu, D. *J. Am. Chem. Soc.* **2006**, *128*, 13058.

(2) Borozdina, Y. B.; Kamm, V.; Laquai, F.; Baumgarten, M. *J. Mater. Chem.* **2012**, *22*, 13260.

(3) Sugawara, T.; Komatsu, H.; Suzuki, K. *Chem. Soc. Rev.* **2011**, *40*, 3105.

(4) (a) Hayes, R. T.; Walsh, C. J.; Wasielewski, M. R. *J. Phys. Chem. A* **2004**, *108*, 2375. (b) Teki, Y.; Miyamoto, S.; Iimura, K.; Nakatsuji, M.; Miura, Y. *J. Am. Chem. Soc.* **2000**, *122*, 984.

(5) Mostovich, E. A.; Borozdina, Y.; Enkelmann, V.; Remović-Langer, K.; Wolf, B.; Lang, M.; Baumgarten, M. *Cryst. Growth Des.* **2012**, *12*, 54.

(6) (a) Morita, Y.; Suzuki, S.; Sato, K.; Takui, T. *Nat. Chem.* **2011**, *3*, 197. (b) Morita, Y.; Nishida, S.; Murata, T.; Moriguchi, M.; Ueda, A.; Satoh, M.; Arifuku, K.; Sato, K.; Takui, T. *Nat. Mater.* **2011**, *10*, 947.

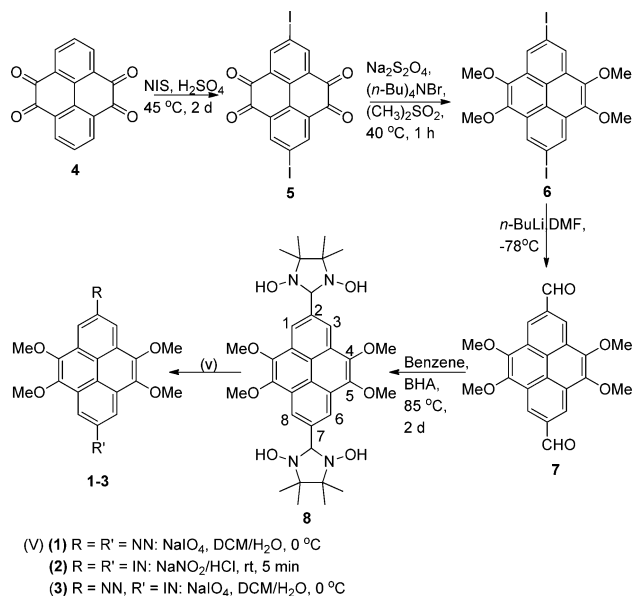
(7) Vaz, M. G. F.; Allao, R. A.; Akpinar, H.; Schlueter, J. A.; Santos, S.; Lahti, P. M.; Novak, M. A. *Inorg. Chem.* **2012**, *51*, 3138.

(8) (a) Ciofini, I.; Adamo, C.; Teki, Y.; Tuyeras, F.; Laine, P. P. *Chem.—Eur. J.* **2008**, *14*, 11385. (b) Giacobbe, E. M.; Mi, Q.; Colvin, M. T.; Cohen, B.; Ramanan, C.; Scott, A. M.; Yeganeh, S.; Marks, T. J.; Ratner, M. A.; Wasielewski, M. R. *J. Am. Chem. Soc.* **2009**, *131*, 3700. (c) Ratera, I.; Veciana, J. *Chem. Soc. Rev.* **2012**, *41*, 303.

positions.<sup>10</sup> Attachment of a radical moiety to the 2,7-positions of pyrene involves a synthetic challenge because the negative electron density at these positions does not allow halogenation. Thus, an alternative synthetic route must be followed to substitute radical moieties at these positions.

Here, we report three 2,7-disubstituted 4,5,9,10-tetra-methoxypyrene-based neutral biradical systems with tunable magnetic exchange interactions by varying the radical moieties at the same positions. The 2,7-disubstituted bis(nitronyl nitroxide) (NN) biradical **1**, bis(imino nitroxide) (IN) biradical **2**, and biradical **3**, which possess both NN and IN radical moieties, were synthesized and characterized by UV-vis, EPR, SQUID, cyclic voltammetry (CV), and single-crystal X-ray diffraction methods. Additionally, the experimental results were verified by DFT calculations.

**Scheme 1.** Synthesis of **1–3**



As shown in Scheme 1, the 2 and 7 positions of pyrene can be activated by oxidizing pyrene to pyrene-4,5,9,10-tetraone, which can undergo efficient halogenation at positions 2 and 7.<sup>11</sup> Further reduction of **5** gave the desired 2,7-diiodotetramethoxypyrene. The precursor for the synthesis of nitronyl or imino nitroxide radical is dialdehyde **8** which was prepared in 71% yield by lithiation of **6** with *n*-BuLi and subsequent addition of DMF at  $-78$  °C. Condensation of **7** with bis(hydroxylamino)dimethylbutane

(BHA) to obtain **8** was performed in benzene at 85 °C. Depending on the oxidizing conditions, biradicals **1–3** were obtained by oxidation of **8**. Upon oxidation of **8** with 2 equiv of NaIO<sub>4</sub> in DCM/H<sub>2</sub>O a two-phase mixture in an ice bath **1** was obtained, while with 3 equiv of NaIO<sub>4</sub> biradical **3** was synthesized. Biradical **2** was prepared by oxidation of **8** with NaNO<sub>2</sub>/HCl at room temperature.

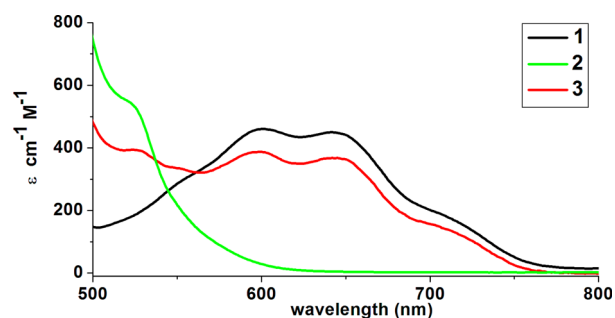
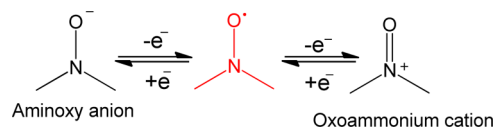


**Figure 1.** Characteristic  $n-\pi^*$  transition of biradicals **1–3** in toluene ( $c = 10^{-4}$  M).

The UV-vis spectrum of neutral radicals gives clear insight of the corresponding radical moieties. The UV-vis spectra of the biradicals **1–3** measured in toluene showed characteristic  $\lambda_{\max}$  due to the  $n-\pi^*$  transition of the radical moiety in the visible range (Figure 1). While the blue biradical **1** carrying two NN moieties absorbs at  $\lambda_{\max} = 601$  nm ( $\epsilon = 460$  cm<sup>-1</sup> M<sup>-1</sup>) and  $\lambda_{\max} = 641$  nm ( $\epsilon = 450$  cm<sup>-1</sup> M<sup>-1</sup>), the orange biradical **2** carrying two IN moieties absorbs at  $\lambda_{\max} = 520$  nm ( $\epsilon = 551$  cm<sup>-1</sup> M<sup>-1</sup>). The gray biradical **3**, which possesses both NN and IN moieties simultaneously, showed characteristic absorption at  $\lambda_{\max} = 599$  nm ( $\epsilon = 389$  cm<sup>-1</sup> M<sup>-1</sup>) and  $\lambda_{\max} = 642$  nm ( $\epsilon = 368$  cm<sup>-1</sup> M<sup>-1</sup>) due to the NN moiety and  $\lambda_{\max} = 524$  nm ( $\epsilon = 393$  cm<sup>-1</sup> M<sup>-1</sup>) stemming from the IN moiety. Therefore, the UV-vis spectra indicate the presence of both radical moieties NN and IN simultaneously in biradical **3**.

**Scheme 2.** Expected Reversible Redox Mechanism



The donor ability of biradicals was investigated by CV. The CV of **1** showed reversible redox waves (Figure S1, Supporting Information) at  $E_{\text{ox}} = 0.95$  V and  $E_{\text{red}} = -0.485$  V versus Ag/Ag<sup>+</sup>, the former can be assigned to resonance delocalization of oxoammonium cation while

(9) (a) Akpınar, H.; Mague, J. T.; Novak, M. A.; Friedman, J. R.; Lahti, P. M. *CrystEngComm* **2012**, *14*, 1515. (b) Teki, Y.; Kimura, M.; Narimatsu, S.; Ohara, K.; Mukai, K. *Bull. Chem. Soc. Jpn.* **2004**, *77*, 95. (c) Miura, Y.; Matsuba, N.; Tanaka, R.; Teki, Y.; Takui, T. *J. Org. Chem.* **2002**, *67*, 8764.

(10) (a) Kreyenschmidt, M.; Baumgarten, M.; Tyutyulkov, N.; Mullen, K. *Angew. Chem., Int. Ed. Engl.* **1994**, *33*, 1957. (b) Karabunarliev, S.; Baumgarten, M. *Chem. Phys.* **2000**, *254*, 239. (c) Suzuki, S.; Takeda, T.; Kuratsu, M.; Kozaki, M.; Sato, K.; Shioimi, D.; Takui, T.; Okada, K. *Org. Lett.* **2009**, *11*, 2816.

(11) Kawano, S.-i.; Baumgarten, M.; Chercka, D.; Enkelmann, V.; Mullen, K. *Chem. Commun* **2013**, *49*, 5058.

(12) Lee, J.; Lee, E.; Kim, S.; Bang, G. S.; Shultz, D. A.; Schmidt, R. D.; Forbes, M. D. E.; Lee, H. *Angew. Chem., Int. Ed.* **2011**, *50*, 4414.

**Table 1.** Optical, Electrochemical, and Magnetic Properties of Biradicals 1–3

	$\lambda_{\max}$ (nm)	$\epsilon$ ( $\text{cm}^{-1}\text{M}^{-1}$ )	$E_{\text{ox}}$ (V) <sup>e</sup>	$E_{\text{red}}$ (V) <sup>b</sup>	$E_{\text{SOMO}}$ (eV) <sup>c</sup>	$E_{\text{LUMO}}$ (eV) <sup>d</sup>	$E_g^{\text{EC}}$ (eV) <sup>i</sup>	$E_g^{\text{OP}}$ (eV) <sup>e</sup>	$\Theta$ (K) <sup>f</sup>	$J_{\text{intra}}$ (K) <sup>g</sup> calcd	$J_{\text{intra}}$ (K) <sup>h</sup> exptl
<b>1</b>	604	460	0.950	-0.485	-5.012	-3.578	1.434	1.614	-4.3	-14.5	-14
	641	450									
<b>2</b>	520	551	1.238	-0.603	-5.600	-3.750	1.850	2.049	-5.7	-3.7	-4.5
<b>3</b>	524	393	0.786 1.246	-0.705	-5.019	-3.526	1.492	1.624	-4.2	-8.0	-9.0
	599	389									
	642	368									

<sup>a,b</sup> 0.1 M of n-Bu<sub>4</sub>NPF<sub>6</sub>, in acetonitrile, Pt electrode, scan rate 100 mV s<sup>-1</sup>. <sup>c,d</sup> Calculated based on formula  $E_{\text{SOMO}} = -(E_{\text{ox,onset}} - E^{(1/2)} \text{Fc}^+/\text{Fc} + 4.8)$  and  $E_{\text{LUMO}} = -(E_{\text{red,onset}} - E^{(1/2)} \text{Fc}^+/\text{Fc} + 4.8)$  eV. <sup>e</sup> Optical energy gap calculated according to the absorption edge. <sup>f</sup> Weiss temperature. <sup>g</sup> Calculated using BLYP/6-31G(d). <sup>h</sup> Calculated using isolated dimer model ( $s = 1/2$ ). <sup>i</sup> Electrochemical energy gap.

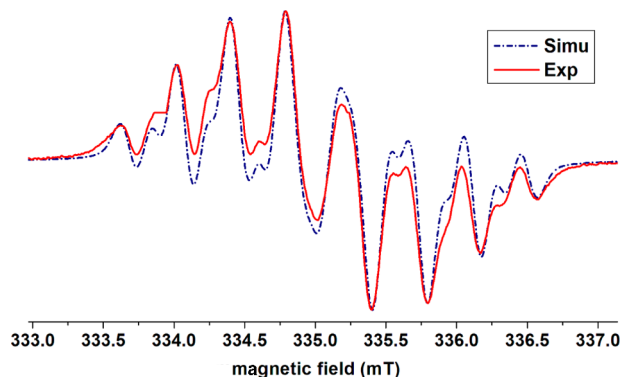
the latter is due to delocalization of aminoxy anion as shown in Scheme 2.<sup>12</sup> The biradical **2** showed nonreversible oxidation<sup>13</sup> wave at  $E_{\text{ox}} = 1.238$  V and reversible reduction wave at  $E_{\text{red}} = -0.603$  V. Interestingly, biradical **3** displayed similar redox behavior as **1** with an additional nonreversible oxidation wave. This nonreversible wave can be assigned to oxidation of the IN radical moiety. As shown in Table 1, the electrochemical band gap is in accordance with the optical band gap. The higher SOMO level of biradicals shows their ability as donor molecule to form charge-transfer complexes.

As magnetic interactions are highly dependent on the geometry and packing of molecules in the crystal lattice,<sup>14</sup> the single crystals of biradicals **1–3**, obtained by slow diffusion of hexane to the solution of biradicals in DCM, were investigated with single-crystal X-ray diffraction. Crystal structure analysis revealed that molecules **1–3** crystallize in the monoclinic  $P21/n$  space group with similar unit cell parameters (Table S3, Supporting Information). Furthermore, they also possess a similar arrangement of molecules in a herringbone pattern (Figure S5, Supporting Information). Thus, it is considered that biradical **1–3** are isomorphous. However, interestingly a significant difference was observed in interplanar spacing. Namely, the shortest  $\pi$ – $\pi$  stacking distance was observed in biradical **1** (3.730 Å) followed by biradical **3** (4.258 Å) and **2** (4.367 Å) (Figure S4, Supporting Information). These differences can be attributed to the influence of the radical moiety on the pyrene core. The torsion angles between the NN moiety and the pyrene ring in **1** are 15° (C3–C4–C11–N1) and 14.8° (C5–C4–C11–N2). The IN moiety in biradical **2** is nearly coplanar with the pyrene ring with a smaller torsion angle of 3.9° (C3–C4–C11–N1). The intermediate torsion angles are observed in biradical **3**, 5.4° (C3–C4–C9–N1) and 4.7° (C5–C4–C9–N2).

(13) (a) Kadirov, M.; Tretyakov, E.; Budnikova, Y.; Valitov, M.; Holin, K.; Gryaznova, T.; Ovcharenko, V.; Sinyashin, O. *J. Electroanal. Chem.* **2008**, *624*, 69. (b) Budnikova, Y. G.; Gryaznova, T. V.; Kadirov, M. K.; Tretyakov, E. V.; Kholin, K. V.; Ovcharenko, V. I.; Sagdeev, R. Z.; Sinyashin, O. G. *Russ. J. Phys. Chem. A* **2009**, *83*, 1976.

(14) (a) Tamura, M.; Nakazawa, Y.; Shiomi, D.; Nozawa, K.; Hosokoshi, Y.; Ishikawa, M.; Takahashi, M.; Kinoshita, M. *Chem. Phys. Lett.* **1991**, *186*, 401. (b) Tamura, M.; Hosokoshi, Y.; Shiomi, D.; Kinoshita, M.; Nakasawa, Y.; Ishikawa, M.; Sawa, H.; Kitazawa, T.; Eguchi, A.; Nishio, Y.; Kajita, K. *J. Phys. Soc. Jpn.* **2003**, *72*, 1735.

The X-band ESR spectra were recorded in oxygen-free toluene at room temperature. The typical ESR spectrum of **1** (Figure S2, Supporting Information) consisted of nine well-resolved lines due to hyperfine coupling (hfc) of two electron spins with four equivalent nitrogen atoms. The experimental spectrum of **1** showed a good agreement with a simulated spectrum considering nitrogen hfc ( $a_{\text{N}}/2$ ) value 0.373 mT (which is half of the hfc observed for mononitronyl nitroxide  $a_{\text{N}} = 0.748$  mT) at  $g = 2.0066$ . The 13-line spectrum of biradical **2** (Figure S2, Supporting Information) was reproduced with hfc values  $a_{\text{N}1}/2 = 0.225$  and  $a_{\text{N}2}/2 = 0.440$  at  $g = 2.0059$ . However, to simulate the nonsymmetric ESR spectra of biradical **3** (Figure 2), three different types of N nuclei and thus hfc values were taken into account: two equivalent N nuclei for the NN unit (with hfc  $a_{\text{N}1}$ ) and two inequivalent N nuclei for the IN unit (with hfc  $a_{\text{N}2}$  and  $a_{\text{N}3}$ ). The best fitting hfc values were  $a_{\text{N}1}/2 = 0.374$  mT for the NN moiety and  $a_{\text{N}2}/2 = 0.200$  and  $a_{\text{N}3}/2 = 0.460$  for the IN moiety with a  $g_{\text{iso}}$  value of 2.0062. The ESR spectra for all biradicals demonstrate that the exchange interactions ( $J$ ) between the radical moieties are much larger than the hyperfine coupling ( $J \gg a_{\text{N}}$ ).

**Figure 2.** X-band ESR spectra of biradical **3** in toluene ( $c = 10^{-4}$  M) at room temperature.

To gain insight into the magnetic exchange interactions, magnetic susceptibilities and magnetizations of polycrystalline samples were measured in the temperature range of

2 K  $\leq T \leq$  300 K using a SQUID magnetometer. As shown in Figure 3, the molar magnetic susceptibility ( $\chi_{\text{mol}}$ ) initially increased with the Curie–Weiss behavior at higher temperature and decreased at lower temperature with a broad peak mainly caused by intramolecular anti-ferromagnetic (AF) interactions. On further lowering the temperature,  $\chi_{\text{mol}}$  decreases close to zero at 2 K which means the biradicals switch from a thermally populated magnetic spin triplet state to a nonmagnetic spin singlet ground state. The intradimer coupling constant  $J_{\text{intra}}$  of R-Py-R' was then estimated using an isolated dimer model<sup>15</sup> ( $H = -2J_{\text{intra}}S_R \cdot S_{R'}$ ). Among the three biradicals, strongest intramolecule exchange interactions thus operate between the NN moieties of biradical **1** ( $J_{\text{intra}} = -14.0$  K) and weakest between the IN moieties of biradical **2** ( $J_{\text{intra}} = -4.5$  K) (Figure S3b, Supporting Information). The intermediate magnetic exchange interactions are obtained by replacing one of the NN moieties in biradical **1** by an IN moiety, i.e., biradical **3** ( $J_{\text{intra}} = -9.0$  K). Moreover, the negative Weiss temperature (Table 1) is observed in all biradicals indicating existence of AF intra- and intermolecular magnetic interactions. The observed effective magnetic moment ( $\mu_{\text{eff}}$ ) values for all biradicals are calculated from temperature dependence of magnetic susceptibility under 0.1 T (inset of Figure 3). At room temperature the magnetic moments are close to the theoretical value  $2.45\mu_{\text{B}}$  for magnetically uncorrelated spins<sup>16</sup> of biradicals.

Moreover, magnetization curves of all biradicals were measured at 2 K (Figure S3, Supporting Information). Whereas the biradicals **1** and **3** showed no applied magnetic field dependence up to 5 T, the biradical **2** showed gradual increase with the increase of the applied magnetic field. This means the biradicals **1** and **3** demonstrate stronger antiferromagnetic intramolecular coupling, keeping the singlet state at 5 T and only the biradical **2** presents a partial switching from singlet to triplet spin state with the applied magnetic fields owing to the small AF interactions.

The intramolecular exchange interaction energies of the biradical species **1–3** were also estimated from the broken-symmetry DFT calculations using X-ray geometry; see Table 1. Good agreement between the latter estimations and the results of magnetic measurements supports the suggested structure of magnetic interactions within the crystalline phase and the experimentally observed trend

(15) Bleaney, B.; Bowers, K. D. *Proc. R. Soc. London A* **1952**, *214*, 451.

(16) Zoppellaro, G.; Enkelmann, V.; Geies, A.; Baumgarten, M. *Org. Lett.* **2004**, *6*, 4929.

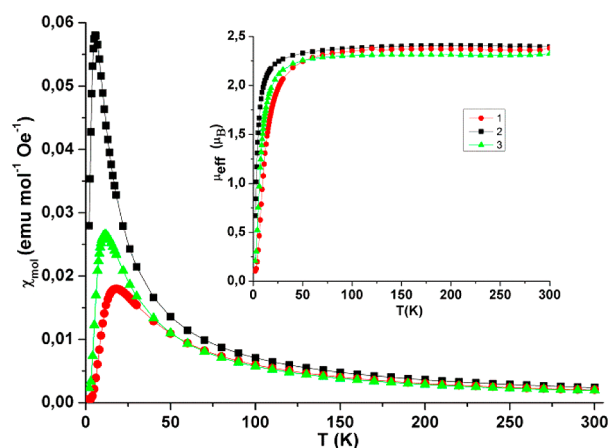


**Figure 3.** Molar magnetic susceptibility,  $\chi_{\text{mol}}$  ( $\text{emu mol}^{-1} \text{Oe}^{-1}$ ) as a function of temperature. Inset: effective magnetic moment,  $\mu_{\text{eff}}$ , as a function of temperature under magnetic field 0.1 T.

in the strength of intramolecular exchange interactions within the biradical family R-Py-R':  $-J_{\text{NN-Py-NN}} > -J_{\text{NN-Py-IN}} > -J_{\text{IN-Py-IN}}$ .

In conclusion, we have demonstrated the first example of 2,7-disubstituted tetramethoxyppyrene-based neutral biradicals with tunable physical and magnetic properties by changing the radical moieties. The experimental  $J$  values are in accordance with the theoretical ones. This is the first report of biradicals possessing NN and IN in the desired 1:1 ratio and not from impurities. We have shown the EPR spectrum of biradical **3** which can be reproduced by spectral simulation using suitable parameters explained in the main text. All three biradicals are very promising candidates to generate photoexcited high spin states and utilization in organic electronics. Such work is underway in our group.

**Acknowledgment.** Support from SFB-TR49 and a scholarship for P.R. are gratefully acknowledged.

**Supporting Information Available.** Full experimental procedures and characterization data. CIF files from the X-ray analysis of **1–3** (CIF). Details of DFT calculations. This material is available free of charge via the Internet at <http://pubs.acs.org>.

The authors declare no competing financial interest.